

Geostationary Satellite Station Keeping and Collocation under High-Thrust Impulsive Control

Pavlašek, Natalia; Di Cairano, Stefano; Weiss, Avishai

TR2025-101 July 09, 2025

Abstract

Ensuring that satellites in geostationary Earth orbit (GEO) remain in their allocated station-keeping windows necessitates accurate station-keeping algorithms. Due to the direct relationship between the fuel efficiency of station-keeping trajectories and satellite mass, optimizing propellant consumption can extend satellite lifetime, increase payload capacity, and lower launch costs. In this paper, we propose a nonlinear model predictive control (NMPC) policy for station keeping and collocation of multiple GEO satellites under infrequent high-thrust impulsive control. We develop a sequential convex programming-based approach to find locally fuel-optimal trajectories with enforced separation distances between collocated satellites. Numerical simulations with NASA's General Mission Analysis Tool demonstrate the effectiveness of the proposed NMPC policy for both GEO satellite station keeping and as a collocation strategy for three GEO satellites in a single station-keeping window.

American Control Conference (ACC) 2025

© 2025 MERL. This work may not be copied or reproduced in whole or in part for any commercial purpose. Permission to copy in whole or in part without payment of fee is granted for nonprofit educational and research purposes provided that all such whole or partial copies include the following: a notice that such copying is by permission of Mitsubishi Electric Research Laboratories, Inc.; an acknowledgment of the authors and individual contributions to the work; and all applicable portions of the copyright notice. Copying, reproduction, or republishing for any other purpose shall require a license with payment of fee to Mitsubishi Electric Research Laboratories, Inc. All rights reserved.

Geostationary Satellite Station Keeping and Collocation under High-Thrust Impulsive Control

Natalia Pavlasek¹, Stefano Di Cairano², and Avishai Weiss³

Abstract—Ensuring that satellites in geostationary Earth orbit (GEO) remain in their allocated station-keeping windows necessitates accurate station-keeping algorithms. Due to the direct relationship between the fuel efficiency of station-keeping trajectories and satellite mass, optimizing propellant consumption can extend satellite lifetime, increase payload capacity, and lower launch costs. In this paper, we propose a nonlinear model predictive control (NMPC) policy for station keeping and collocation of multiple GEO satellites under infrequent high-thrust impulsive control. We develop a sequential convex programming-based approach to find locally fuel-optimal trajectories with enforced separation distances between collocated satellites. Numerical simulations with NASA’s General Mission Analysis Tool demonstrate the effectiveness of the proposed NMPC policy for both GEO satellite station keeping and as a collocation strategy for three GEO satellites in a single station-keeping window.

I. INTRODUCTION

Satellites in geostationary Earth orbit (GEO) require station keeping in order to counteract orbital perturbation-induced drift. Early GEO station-keeping methods determined the thrust requirements for maintaining a satellite in a station-keeping window analytically, by directly compensating for drift in orbital elements [1]–[3]. These methods require manual operation and are not necessarily fuel-optimal. Recently, work on station keeping has focused on optimization-based approaches for satellites equipped with low-thrust electric propulsion, see [4]–[7] and references therein. Due to the low-thrust magnitudes of electric propulsion, and thus the relatively high frequency of the required station-keeping maneuvers, optimization-based station-keeping methods for low-thrust satellites use relatively short prediction horizons to keep the size of the optimization problem manageable.

In contrast, satellites equipped with chemical propulsion systems apply thrust with approximately 100 times the magnitude of low-thrust systems [8]. The high thrust magnitude enables these satellites to apply thrust less frequently. However, infrequent station-keeping maneuvers mean that optimization-based station-keeping algorithms must predict the motion of the satellite accurately for long periods of time, without the ability to compensate for modeling errors using feedback [9], [10]. Comparatively less research has

been performed in this area in recent years. To ensure that their satellite prediction models are accurate, the methods in [9], [10] constrain the satellite to remain near the trajectory about which the dynamics are linearized. Such a constraint is conservative, as it encourages the satellite to stay near the center of the station-keeping window.

The problem of positioning multiple satellites in the same station-keeping window, referred to as *collocation*, introduces additional complexity; collocated satellites must maintain suitable distance from one another. One approach for GEO collocation separates the group of satellites by eccentricity and inclination such that the satellites occupy slightly different orbits with low probability of collision [11], [12]. Eccentricity and inclination separation constrains each satellite to occupy only a subset of the allocated station-keeping window, and as such is a conservative approach. More recent methods for GEO collocation use optimization-based techniques [10], [13], but are typically only applicable to satellites with low-thrust propulsion.

Recent advances in trajectory optimization lend themselves well to high-thrust satellite station keeping and collocation. Exact discretization methods [14], [15] provide highly accurate linear dynamics models that can be used within the sequential convex programming (SCP) framework to provide a local solution to a nonconvex optimization problem [16], [17]. Recently, the use of an isoperimetric constraint reformulation within an SCP-based framework has been shown to provide continuous-time constraint satisfaction, allowing coarse time discretization [18]. These methods can be used within the model predictive control (MPC) framework [19]. MPC is a receding-horizon control strategy that exploits a model of the system dynamics to determine a control trajectory and corresponding state trajectory that is optimal with respect to an objective function, subject to constraints [20].

In this paper, we propose a nonlinear MPC policy for station keeping and collocation under high-thrust impulsive control. We use SCP to solve for optimal control inputs, while considering the nonconvex dynamics and constraints. Time dilation [18], [21]–[24] is used to make thruster firing time a problem variable. We additionally apply the constraint reformulation described in [18] to enforce satellite separation distance between discrete-time samples of the position trajectory in a three-satellite collocation scenario. We use NASA’s General Mission Analysis Tool (GMAT) in order to validate and assess the performance of our control strategy. Our simulations close the loop between the proposed MPC policy and the GMAT propagator; the MPC policy computes

¹N. Pavlasek is with the William E. Boeing Department of Aeronautics and Astronautics, University of Washington, Seattle, WA 98195. E-mail: pavlasek@uw.edu. She interned at MERL during the development of this work.

^{2,3}S. Di Cairano and A. Weiss are with Mitsubishi Electric Research Laboratories (MERL), Cambridge, MA 02139, USA. Emails: {dicairano, weiss} at merl.com

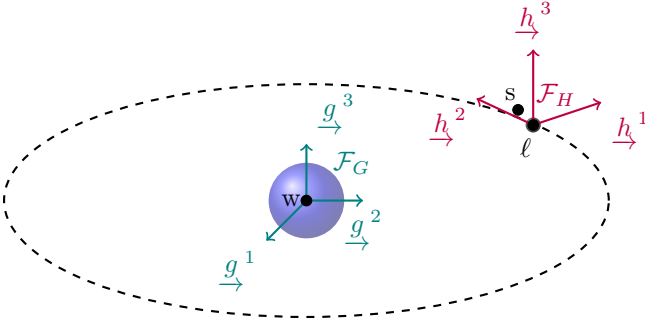


Fig. 1: Illustration of satellite orbiting the Earth with J2000 inertial frame, \mathcal{F}_G and Hill frame, \mathcal{F}_H .

optimal control inputs, which are then applied to a satellite and propagated through GMAT. The propagated satellite state is then used to initialize the controller during the next MPC period.

The remainder of this paper is organized as follows. Section II introduces the concepts used in the proposed fuel-optimal station-keeping formulation, which is introduced in Section III. The problem is extended to satellite collocation in Section IV. Section V presents results. Finally, concluding remarks are given in Section VI.

A. Notation

The following notation is used throughout this work. A frame \mathcal{F}_A is defined by three orthonormal basis vectors $\{\underline{a}^1, \underline{a}^2, \underline{a}^3\}$. The physical vector \underline{r} resolved in \mathcal{F}_A is denoted by \mathbf{r}_A . The relationship between \mathbf{r}_A and \mathbf{r}_B is $\mathbf{r}_A = \mathbf{C}_{AB}\mathbf{r}_B$, where $\mathbf{C}_{AB} \in SO(3)$. The physical vector describing the position of point c relative to point d is denoted by \underline{r}^{cd} . The time derivative of \underline{r}^{cd} with respect to frame A is denoted $\underline{v}^{cd/A} = \dot{\underline{r}}^{cd \cdot A}$. The $n \times n$ identity matrix is denoted \mathbf{I}_n , and the $n \times m$ matrix of zeros is denoted $\mathbf{0}_{n \times m}$. We denote the number of elements in vector \mathbf{z} by n_z . The set of real numbers and non-negative real numbers are denoted by \mathbb{R} and \mathbb{R}_+ , respectively. Given a continuous-time signal $x(t)$ sampled with period ΔT , we denote the value of the signal at time instant $k\Delta T$, $k \in \{1, \dots, K\}$, by $x_k = x(k\Delta T)$.

II. PROBLEM MODELLING

We consider the development of a controller that maintains a GEO satellite within a range of longitudes and latitudes, which define a station-keeping window.

A. Satellite model

Consider the J2000 inertial frame, denoted \mathcal{F}_G , and the Hill frame, \mathcal{F}_H , defined by the basis vectors $\{\underline{h}^1, \underline{h}^2, \underline{h}^3\}$, where \underline{h}^1 is aligned with the nominal GEO orbital radius, \underline{h}^3 is orthogonal to the orbital plane, and \underline{h}^2 completes the right-handed coordinate frame depicted in Figure 1. We assume the existence of an unforced particle w located at the center of the Earth, and denote a point at the center of mass of the GEO satellite by s. For the purposes of

defining a station-keeping window, introduced in Section II-B, it is useful to define a reference point ℓ that moves along a nominal Keplerian geostationary orbit. The translational equation of motion for the satellite relative to the inertial frame \mathcal{F}_G is given by

$$\ddot{\underline{r}}^{sw}(t) = -\mu^{\text{earth}} \frac{\underline{r}^{sw}(t)}{\|\underline{r}^{sw}(t)\|_2^3} + \underline{a}^{\text{pert}}(t) + \underline{a}^{\text{ctrl}}(t), \quad (1)$$

where $\underline{r}^{sw} : \mathbb{R}_+ \rightarrow \mathbb{R}^3$ is the position trajectory of s relative to w, $\mu^{\text{earth}} \in \mathbb{R}$ is the standard gravitational parameter of the Earth, $\underline{a}^{\text{pert}} : \mathbb{R}_+ \rightarrow \mathbb{R}^3$ is the acceleration induced by perturbing forces, and $\underline{a}^{\text{ctrl}} : \mathbb{R}_+ \rightarrow \mathbb{R}^3$ is the input applied to the satellite.

We consider perturbing accelerations from three sources: gravitational forces between the Sun and the Moon and the satellite, solar radiation pressure, and Earth's non-Keplerian gravitational potential. Gravitational forces between the Sun and Moon and the satellite result in a perturbing acceleration applied to the satellite, computed according to

$$\underline{a}^{\text{grav},j}(t) = \mu^j \left(\frac{\underline{r}^{jw}(t) - \underline{r}^{sw}(t)}{\|\underline{r}^{jw}(t) - \underline{r}^{sw}(t)\|_2^3} - \frac{\underline{r}^{jw}(t)}{\|\underline{r}^{jw}(t)\|_2^3} \right), \quad (2)$$

where $j \in \{\text{sun}, \text{moon}\}$, and $\mu^j \in \mathbb{R}$ is the standard gravitational parameter of body j . The impact of photons with the satellite results in an acceleration due to solar radiation pressure, computed as [25]

$$\underline{a}^{\text{srp}}(t) = \frac{p^{\text{s.r.}} c^{\text{refl}} s^{\text{facing}}}{m^s} \frac{\underline{r}^{\text{sun,w}}(t) - \underline{r}^{sw}(t)}{\|\underline{r}^{\text{sun,w}}(t) - \underline{r}^{sw}(t)\|_2}, \quad (3)$$

where $p^{\text{s.r.}} \in \mathbb{R}$ is the flux pressure, computed as $p^{\text{s.r.}} = \frac{p_0}{c}$, where $p_0 = 1367.0 \frac{\text{W}}{\text{m}^2}$ is the solar constant, and $c = 299792458 \frac{\text{m}}{\text{s}}$ is the speed of light, $c^{\text{refl}} \in \mathbb{R}$ is the reflectivity constant, $s^{\text{facing}} \in \mathbb{R}$ is the Sun-facing area, and $m^s \in \mathbb{R}$ is the satellite mass. Earth's oblateness results in a non-uniform gravitational potential, defined by spherical harmonic functions, which induces an additional perturbing acceleration, $\underline{a}^{\text{s.h.}}$ [26]. Spherical harmonic gravitational potential terms up to the 10th order are computed using [27]. The resulting perturbing acceleration is

$$\underline{a}^{\text{pert}} = \underline{a}^{\text{grav,sun}} + \underline{a}^{\text{grav,moon}} + \underline{a}^{\text{srp}} + \underline{a}^{\text{s.h.}}. \quad (4)$$

We assume the satellite is actuated by impulsive accelerations, resulting in instantaneous velocity changes Δv . The acceleration input $\underline{a}^{\text{ctrl}}(t)$ in (1) is given by

$$\underline{a}^{\text{ctrl}}(t) = \delta(t) \underline{u}(t), \quad (5)$$

where $\underline{u} : \mathbb{R}_+ \rightarrow \mathbb{R}^3$ is the control input, and $\delta(t)$ is the Dirac delta function.

We define the satellite's state to be the concatenation of its position and velocity, both resolved in \mathcal{F}_G , so that the

state trajectory $\mathbf{x} : \mathbb{R}_+ \rightarrow \mathbb{R}^6$ is

$$\mathbf{x}(t) = \begin{bmatrix} \mathbf{r}_G^{\text{sw}}(t) \\ \mathbf{v}_G^{\text{sw}/G}(t) \end{bmatrix}, \quad (6)$$

where $\mathbf{v}_G^{\text{sw}/G}(t)$ is the time derivative of $\mathbf{r}_G^{\text{sw}}(t)$, taken with respect to frame \mathcal{F}_G , resolved in \mathcal{F}_G . The system dynamics are given by

$$\dot{\mathbf{x}}(t) = \begin{bmatrix} \mathbf{v}_G^{\text{sw}/G} \\ -\mu^{\text{earth}} \frac{\mathbf{r}_G^{\text{sw}}}{\|\mathbf{r}_G^{\text{sw}}\|_2^3} + \mathbf{a}_G^{\text{pert}} + \delta(t)\mathbf{u}_G \end{bmatrix}, \quad (7a)$$

$$= \mathbf{f}(t, \mathbf{x}, \mathbf{u}), \quad (7b)$$

where we have defined $\mathbf{u} = \mathbf{u}_G$.

B. Station keeping

The station-keeping window can be described relative to reference point ℓ . We make the following assumption.

Assumption 1. *The distance between the satellite and reference point ℓ , projected onto \underline{h}^1 is small.*

Assumption 1 enables the translation from longitudinal and latitudinal constraints to box constraints on the satellite position relative to the position of reference point ℓ , resolved in \mathcal{F}_H . Given the maximum deviation from the nominal longitude, $\lambda_1^{\text{max}} \in \mathbb{R}$, and the maximum deviation from the nominal latitude, $\lambda_2^{\text{max}} \in \mathbb{R}$, the station-keeping constraint can be expressed as

$$|\mathbf{r}_{H,i}^{\text{sw}}(t) - \mathbf{r}_{H,i}^{\ell w}(t)| \leq a_0 \tan \lambda_{i-1}^{\text{max}}, \quad i \in \{2, 3\}, \quad (8)$$

where $a_0 \in \mathbb{R}$ is the semi-major axis of the nominal geostationary orbit, and $\mathbf{r}_{H,i}^{jw}(t)$ is the i^{th} element of $\mathbf{r}_H^{jw}(t)$, $j \in \{s, \ell\}$.

C. Sequential convex programming

We employ the prox-linear method [28], which is closely related to the penalized trust region (PTR) algorithm [21], [29], to solve the nonconvex problem of finding a fuel-minimizing trajectory under the nonconvex dynamics given in (7).

D. Time dilation

Time dilation can be used to transform a free-final-time optimal control problem (OCP) to an equivalent fixed-final-time problem [18], [21]–[24]. Let t be a strictly increasing, continuously-differentiable mapping $t : [0, 1] \rightarrow \mathbb{R}_+$, with boundary conditions $t(0) = t_i$, $t(1) = t_f$. The derivative of the map is

$$s(\tau) = \frac{dt(\tau)}{d\tau}, \quad (9)$$

where $\tau \in [0, 1]$. We refer to s as the *dilation factor*, and treat it as a control input, and augment the state with time. The augmented control input and augmented states are defined as

$$\tilde{\mathbf{u}}(\tau) = \begin{bmatrix} \mathbf{u}(\tau) \\ s(\tau) \end{bmatrix}, \quad \tilde{\mathbf{x}}(\tau) = \begin{bmatrix} \mathbf{x}(\tau) \\ t(\tau) \end{bmatrix}. \quad (10)$$

We denote a derivative with respect to τ as $\overset{\circ}{\square}$. The dynamics in (7) can be expressed with respect to τ , as

$$\overset{\circ}{\tilde{\mathbf{x}}} = \frac{d\tilde{\mathbf{x}}}{dt} \frac{dt(\tau)}{d\tau}, \quad (11a)$$

$$= \begin{bmatrix} \mathbf{f}(t(\tau), \mathbf{x}(\tau), \mathbf{u}(\tau)) \\ 1 \end{bmatrix} s(\tau), \quad (11b)$$

$$=: \mathbf{f}^s(\tilde{\mathbf{x}}(\tau), \tilde{\mathbf{u}}(\tau)), \quad (11c)$$

where $\mathbf{f}^s : \mathbb{R}^{n_x} \times \mathbb{R}_+ \times \mathbb{R}^{n_u} \times \mathbb{R} \rightarrow \mathbb{R}^{n_x+1}$.

E. Parametrization and time discretization

The dynamics in (11) and constraints in (8) result in an infinite-dimensional OCP. To form a tractable numerical OCP, we time-discretize the system to obtain a finite-dimensional nonconvex OCP. We propose a direct method that uses an inverse-free exact discretization scheme referred to as multiple-shooting [30] to solve the OCP. We parameterize the augmented control using a zero-order hold.

We first note that the continuous-time dynamics in (11) can equivalently be expressed as

$$\tilde{\mathbf{x}}_{k+1} = \tilde{\mathbf{x}}_k + \int_{\tau_k}^{\tau_{k+1}} \mathbf{f}^s(\tilde{\mathbf{x}}(\tau), \tilde{\mathbf{u}}(\tau)) d\tau, \quad (12)$$

where $\tilde{\mathbf{x}}_k$ is the augmented state sampled at τ_k . We start by computing the partial derivatives of the dynamics in (11), to obtain

$$\bar{\mathbf{A}}(\tau) = \left. \frac{\partial \mathbf{f}^s(\tilde{\mathbf{x}}, \tilde{\mathbf{u}})}{\partial \tilde{\mathbf{x}}} \right|_{\tilde{\mathbf{x}}(\tau), \tilde{\mathbf{u}}(\tau)}, \quad \bar{\mathbf{B}}(\tau) = \left. \frac{\partial \mathbf{f}^s(\tilde{\mathbf{x}}, \tilde{\mathbf{u}})}{\partial \tilde{\mathbf{u}}} \right|_{\tilde{\mathbf{x}}(\tau), \tilde{\mathbf{u}}(\tau)},$$

where $\bar{\mathbf{A}} : [0, 1] \rightarrow \mathbb{R}^{n_{\tilde{\mathbf{x}}} \times n_{\tilde{\mathbf{x}}}}$, $\bar{\mathbf{B}} : [0, 1] \rightarrow \mathbb{R}^{n_{\tilde{\mathbf{x}}} \times n_{\tilde{\mathbf{u}}}}$, and $\tilde{\mathbf{x}}(\tau)$ and $\tilde{\mathbf{u}}(\tau)$ are the state and control trajectories, respectively, about which the dynamics are linearized.

Consider the initial value problem

$$\overset{\circ}{\Phi}_{\tilde{\mathbf{x}}}(\tau, \tau_k) = \bar{\mathbf{A}}(\tau) \Phi_{\tilde{\mathbf{x}}}(\tau, \tau_k), \quad (13a)$$

$$\overset{\circ}{\Phi}_{\tilde{\mathbf{u}}}(\tau, \tau_k) = \bar{\mathbf{A}}(\tau) \Phi_{\tilde{\mathbf{u}}}(\tau, \tau_k) + \bar{\mathbf{B}}(\tau), \quad (13b)$$

$$\Phi_{\tilde{\mathbf{x}}}(\tau_k, \tau_k) = \mathbf{I}_{n_{\tilde{\mathbf{x}}}}, \quad (13c)$$

$$\Phi_{\tilde{\mathbf{u}}}(\tau_k, \tau_k) = \mathbf{0}_{n_{\tilde{\mathbf{x}}} \times n_{\tilde{\mathbf{u}}}}. \quad (13d)$$

Equation (13) can be solved to obtain

$$\bar{\mathbf{A}}_k = \Phi_{\tilde{\mathbf{x}}}(\tau_{k+1}, \tau_k), \quad (14a)$$

$$\bar{\mathbf{B}}_k = \Phi_{\tilde{\mathbf{u}}}(\tau_{k+1}, \tau_k), \quad (14b)$$

$$\bar{\mathbf{z}}_k = \tilde{\mathbf{x}}(\tau_{k+1}) - \bar{\mathbf{A}}_k \tilde{\mathbf{x}}_k - \bar{\mathbf{B}}_k \tilde{\mathbf{u}}_k. \quad (14c)$$

where $\bar{\mathbf{A}}_k \in \mathbb{R}^{n_{\tilde{\mathbf{x}}} \times n_{\tilde{\mathbf{x}}}}$, and $\bar{\mathbf{B}}_k \in \mathbb{R}^{n_{\tilde{\mathbf{x}}} \times n_{\tilde{\mathbf{u}}}}$.

The discrete-time linear dynamics are then given by

$$\tilde{\mathbf{x}}_{k+1} \approx \bar{\mathbf{A}}_k \tilde{\mathbf{x}}_k + \bar{\mathbf{B}}_k \tilde{\mathbf{u}}_k + \bar{\mathbf{z}}_k. \quad (15)$$

F. Continuous-time constraint satisfaction

Direct methods for trajectory optimization typically enforce constraints at discrete sample points, $\mathbf{x}_k = \mathbf{x}(t_k)$, with $k \in \{0, \dots, K\}$, which allows for inter-sample constraint violation, or the violation of constraints between samples [18], [24]. In contrast, methods with isoperimetric constraint reformulation [18], [24] impose constraints as path

constraints, which are enforced along the full trajectory. Consider the constraint function $g : \mathbb{R}_+ \times \mathbb{R}_{n_x} \times \mathbb{R}_{n_u} \rightarrow \mathbb{R}$, and the penalty function

$$\Lambda(t, \mathbf{x}(t), \mathbf{u}(t)) = \max\{0, g(t, \mathbf{x}(t), \mathbf{u}(t))\}^2. \quad (16)$$

Constraint $g(t, \mathbf{x}(t), \mathbf{u}(t)) \leq 0$ is satisfied almost everywhere in $[t_i, t_f]$ if and only if

$$\int_{t_i}^{t_f} \Lambda(t, \mathbf{x}(t), \mathbf{u}(t)) dt = 0. \quad (17)$$

We introduce $y : \mathbb{R}_+ \rightarrow \mathbb{R}$ with dynamics and boundary value

$$\dot{y}(t) = \Lambda(t, \mathbf{x}(t), \mathbf{u}(t)), \quad (18a)$$

$$y(0) = y(t_f), \quad (18b)$$

which accumulates constraint violation. Within an OCP, (18a) is imposed by augmenting the vehicle dynamics with state y .

Applying time dilation, as discussed in Section II-D, yields

$$\dot{y}(\tau) = s(\tau)\Lambda(\tilde{\mathbf{x}}(t(\tau)), \tilde{\mathbf{u}}(t(\tau))), \quad (19a)$$

$$y(0) = y(1). \quad (19b)$$

As discussed in [18], in order to satisfy the linear independence constraint qualification (LICQ), (19b) is enforced as

$$y(1) - y(0) \leq \epsilon^y, \quad (20)$$

where $\epsilon^y \in \mathbb{R}$ is a numerically significant but physically insignificant quantity. See [18] for details.

III. SATELLITE STATION KEEPING

The control architecture can now be described. We develop a receding-horizon nonlinear MPC policy that uses SCP to solve for state and control trajectories. The control input is infrequent and impulsive, and is constrained to be in the east-west (EW) direction, along \underline{h}_x^2 , and in the north-south (NS) direction, along \underline{h}_y^3 .

A. Maneuver timing

We consider a satellite equipped with a chemical propulsion system, which has fixed-directional thrust with restricted firing times. We define the thrust to be an impulsive acceleration, and denote the set of times at which north-south (NS) thrust is applied by \mathcal{T}^{NS} , and the set of times at which east-west (EW) thrust is applied by \mathcal{T}^{EW} . We define the *control period* to be a user-defined period of time in which a specified number of NS-pointing thruster firings, n^{NS} , and of EW-pointing thruster firings, n^{EW} , can occur.

In order to make firing time a free variable, we apply time dilation, as introduced in Section II-D. In this framework, thrust is applied at fixed intervals in dilated-time space, however the corresponding true times are made free through the mapping from dilated time to true time.

B. Station keeping as a nonconvex optimization problem

We make the following assumption, which enables the use of state-independent rotation matrices.

Assumption 2. *The rotation from the inertial frame, \mathcal{F}_G , to the Hill frame, \mathcal{F}_H , is a good approximation for the rotation from the inertial frame to the satellite orbit frame.*

The continuous-time OCP of minimizing fuel, subject to time-dilated dynamics (11c), initial condition, and station-keeping constraint (8), can be expressed as

$$\min_{\tilde{\mathbf{u}}(\tau), \tilde{\mathbf{x}}(\tau)} \|\mathbf{u}(\tau)\|_1 \quad (21a)$$

$$\text{s.t. } \dot{\tilde{\mathbf{x}}}(\tau) = \mathbf{f}^s(\tilde{\mathbf{x}}(\tau), \tilde{\mathbf{u}}(\tau)), \forall \tau \in [0, 1], \quad (21b)$$

$$\tilde{\mathbf{x}}(0) = \tilde{\mathbf{x}}_0, \quad (21c)$$

$$\left| \mathbf{C}_{HG}^{i,:}(\tau) (\mathbf{r}_G^{\text{sw}}(\tau) - \mathbf{r}_G^{\ell\text{w}}(\tau)) \right| \leq a_0 \tan \lambda_{i-1}^{\max}, \quad \tau \in [0, 1], i \in \{2, 3\}, \quad (21d)$$

where $\mathbf{C}_{HG}^{i,:}$ denotes the i^{th} row of the rotation matrix that transforms vectors in \mathcal{F}_G into \mathcal{F}_H , and the dynamics in (21b) are defined by (11b) and (7a).

C. Discrete-time convex subproblem

Problem (21) is infinite-dimensional since the states are continuous-time quantities. The problem must be time-discretized in order to solve it numerically. We use the discretization scheme presented in II-E to discretize (21b). In the discrete-time system, the impulsive acceleration in (7a) becomes a step input in velocity.

We define \mathcal{I}^{NS} and \mathcal{I}^{EW} to be the indices at which the thrust firing times $t \in \mathcal{T}^{\text{NS}}$ and $t \in \mathcal{T}^{\text{EW}}$ occur. Using SCP, we express the convex subproblem as

$$\min_{\tilde{\mathbf{u}}_{0:K-1}, \tilde{\mathbf{x}}_{0:K}} \sum_{k=0}^{K-1} (\|\mathbf{u}_k\|_2 + w^{\text{dyn}} \|\boldsymbol{\nu}_k\|_1 + w^{\text{sk}} \|\gamma_k\|_1 + w^{\text{tr},\mathbf{x}} \|\tilde{\mathbf{x}}_k - \bar{\tilde{\mathbf{x}}}_k\|_2^2 + w^{\text{tr},s} \|s_k - \bar{s}_k\|_2^2) \quad (22a)$$

$$\text{s.t. } \boldsymbol{\nu}_k = \bar{\mathbf{A}}_k \tilde{\mathbf{x}}_k + \bar{\mathbf{B}}_k^s s_k + \mathbb{1}_{\mathcal{I}^{\text{EW}}}(k) \bar{\mathbf{B}}_k^{\text{EW}} u_k^{\text{EW}} + \mathbb{1}_{\mathcal{I}^{\text{NS}}}(k) \bar{\mathbf{B}}_k^{\text{NS}} u_k^{\text{NS}} + \bar{\mathbf{z}}_k - \tilde{\mathbf{x}}_{k+1}, \quad k \in \{0, \dots, K\}, \quad (22b)$$

$$\tilde{\mathbf{x}}_0 = \tilde{\mathbf{x}}_0, \quad (22c)$$

$$\left| \mathbf{C}_{HG}^{i,:}(\tau) (\mathbf{r}_G^{\text{skw}} - \mathbf{r}_G^{\ell\text{kw}}) \right| - a_0 \tan \lambda_{i-1}^{\max} \leq \gamma_{k-1}^1, \quad k \in \{1, \dots, K\}, i \in \{2, 3\}, \quad (22d)$$

where $w^{\text{dyn}} \in \mathbb{R}$, $w^{\text{sk}} \in \mathbb{R}$, $w^{\text{tr},\mathbf{x}} \in \mathbb{R}$, and $w^{\text{tr},s} \in \mathbb{R}$ are user-selected dynamics, station-keeping, state trust-region, and time-dilation factor trust-region weights, respectively, and we have defined $\bar{\mathbf{B}}_k^{\text{EW}}$ to be the column of $\bar{\mathbf{B}}_k$ corresponding to EW thrust, $\bar{\mathbf{B}}_k^{\text{NS}}$ to be the column of $\bar{\mathbf{B}}_k$ corresponding to NS thrust, and $\bar{\mathbf{B}}_k^s$ to be the column of $\bar{\mathbf{B}}_k$ corresponding to the dilation factor. The indicator function $\mathbb{1}_{\mathcal{I}_j}(k)$, $j \in \{\text{EW}, \text{NS}\}$ evaluates to 1 if $k \in \mathcal{I}_j$, and to 0 otherwise. The station-keeping constraints (22d) are imposed

with slack variables to allow minimal violation of the station-keeping constraint. This prevents the optimization problem from prioritizing satisfying the station-keeping constraint while sacrificing dynamic feasibility.

D. Model predictive control

The GEO station-keeping problem is solved over long horizons, with uncontrolled periods of several days. We use MPC to determine optimal control inputs over a receding horizon, and to provide feedback to the system.

For each MPC period, (21) is solved locally by iteratively solving (22), linearized about the previous solution, $(\bar{\mathbf{x}}, \bar{\mathbf{u}})$, to convergence. The system is propagated using GMAT for time $[t_i, t^{\text{app}}]$, where $t^{\text{app}} < t_f$ with the control inputs found by solving the OCP. The state of the system at the end of the propagation becomes the initial state $\bar{\mathbf{x}}_0$ in Problem (21) for the next MPC period.

IV. SATELLITE COLLOCATION

The algorithm proposed in Section III can be extended to the problem of collocating multiple satellites in a single station-keeping window. In order to maintain suitable distance between satellites, a pairwise separation constraint is added to Problem (21). For each pair of satellites, s^i and s^j , the nonconvex pairwise separation constraint is given by

$$\left\| \mathbf{r}_G^{s^i w}(t) - \mathbf{r}_G^{s^j w}(t) \right\|_2 \geq d^{\min}, \quad (23)$$

where s^i is a point at the center of mass of satellite i , and $d^{\min} \in \mathbb{R}$ is the minimum allowable separation distance between two satellites. Constraint (23) can be linearized and enforced at $\{t_1, t_2, \dots, t_K\}$ using the SCP framework. However, in the proposed problem formulation, the long MPC prediction horizons and infrequent control demands coarse sampling periods, such that the problem is optimized over states occurring several hours apart. Due to the risk of satellite collisions between samples, we adopt the framework in [18], where (23) is subjected to an isoperimetric reformulation to avoid inter-sample constraint violation.

Consider the penalty function $\Lambda : \mathbb{R}_+ \times \mathbb{R}^{2n_r} \rightarrow \mathbb{R}_+$

$$\Lambda(t, \mathbf{r}_G^{s^i w}, \mathbf{r}_G^{s^j w}) = \max \{0, d^{\min} - \|\mathbf{r}_G^{s^i w} - \mathbf{r}_G^{s^j w}\|_2\}^2. \quad (24)$$

Using the formulation described in Section II-F, we augment the dynamics in (7) with (19a) and (24), and enforce (19b) in the OCP. This framework enforces satisfaction of (23) at all points in the trajectory at SCP convergence.

V. GEO SATELLITE RESULTS

We demonstrate the proposed algorithm in simulation using GMAT. Results for single-satellite station keeping and three-satellite collocation are presented. In both cases, an MPC policy is used. We consider a scenario in which the satellite has a two-week control cycle, during which its north-south (NS) thruster can fire once, and its east-west (EW) thruster can fire twice. The thrust is assumed to result in an instantaneous change in the satellite's velocity. The

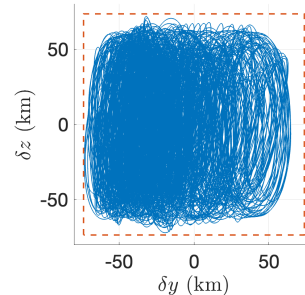


Fig. 2: Satellite position relative to the center of the station-keeping window, resolved in \mathcal{F}_H (blue) over 504 day period, with station-keeping window boundary (orange).

maximum deviation from the nominal latitude and longitude is $\lambda_1^{\max} = \lambda_2^{\max} = 0.1^\circ$, so that the station-keeping window measures 0.2° in latitude and longitude. We use a time-discretization step of 8 hours. The constants used to compute the solar radiation pressure are $c^{\text{refl}} = 1.09$, $s^{\text{facing}} = 50 \text{ m}^2$, and $m^s = 2500 \text{ kg}$.

A. Single-satellite station keeping

We first demonstrate the proposed algorithm on a single-satellite station-keeping scenario. An MPC horizon of 16 weeks is used to compute the control inputs applied to the satellite. Once computed, the system is propagated for 2 weeks, before recomputing the control inputs. The simulation is performed over 504 days.

Figure 2 shows the position of the satellite relative to the center of the station-keeping window, resolved in the Hill frame. The dashed line represents the boundary of the station-keeping window. The satellite remains inside the station-keeping window throughout the simulation.

Figure 3 shows the cumulative control input over time. The annual Δv in the EW direction is $1.8 \frac{\text{m}}{\text{s}}$ for the first 365 days, and $1.9 \frac{\text{m}}{\text{s}}$ for the last 365 days. In the NS direction, the annual Δv is $50.2 \frac{\text{m}}{\text{s}}$ for the first 365 days and $53.8 \frac{\text{m}}{\text{s}}$ for the last 365 days. The total Δv requirement is therefore $52.0 \frac{\text{m}}{\text{s}}$ for the first 365 days and $55.7 \frac{\text{m}}{\text{s}}$.

B. Three-satellite collocation

We demonstrate the proposed algorithm for satellite collocation with three satellites. As in the single-satellite station-keeping scenario, an MPC horizon of 16 weeks is used, and the system is propagated for two weeks. The minimum separation distance between any two satellites is constrained to be 2 km. We compare performance of the proposed algorithm with the separation constraint applied with the constraint reformulation framework described in Section IV to a baseline with the separation constraint applied only at the discrete time steps. We choose to apply the separation constraint (23) with the constraint reformulation framework and the station-keeping constraint (8) at the discrete sample points since a collision between satellites is mission-critical.

Figure 4 shows the separation distance between each pair of satellites, with the pairwise separation constraint (23)

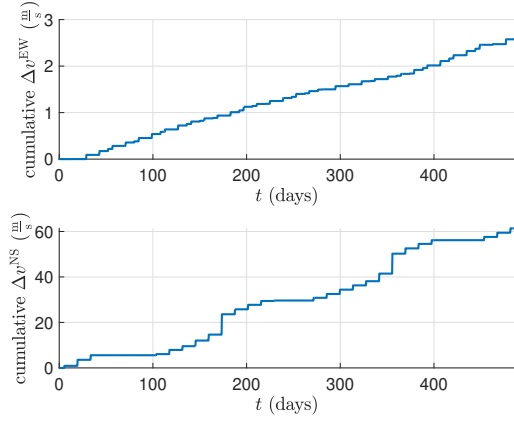


Fig. 3: Cumulative control input in EW and NS directions for satellite station keeping over 504 day period.

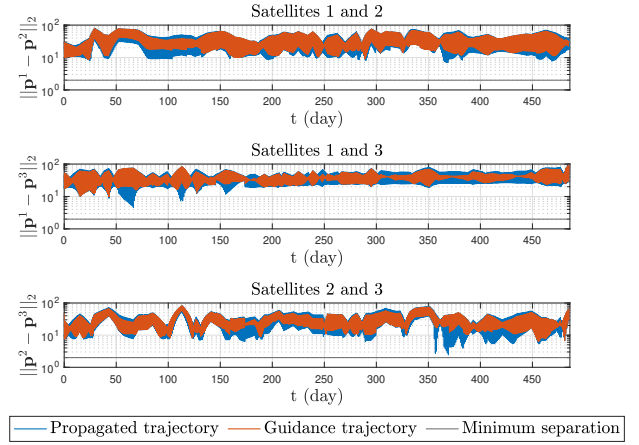
applied with the isoperimetric constraint reformulation (Figure 4a) and applied only at the sample points (Figure 4b). The guidance trajectory (orange) is the output of the optimizer, in which the states are time-discretized with 8 hours between samples. The propagated trajectory (blue) is the result of propagating the nonlinear dynamics using GMAT. Figure 4a shows that when the separation constraint is applied with the isoperimetric constraint reformulation, the nonlinear propagation of the satellite trajectories satisfy the pairwise-separation constraint. Figure 4b shows that with the separation constraint applied only at the discrete sample points, several close approaches between satellites 1 and 2, and satellites 2 and 3 occur. The closest approach occurs between satellites 1 and 2 at just 0.39 km apart.

Figure 5 shows the position of each of the three satellites relative to the center of the station-keeping window, resolved in \mathcal{F}_H , with the pairwise separation constraint (23) applied using the isoperimetric constraint reformulation (Figure 5a), and applied only at the sample points (Figure 5b). The station-keeping window boundary is denoted by the orange dashed line. Note that since the station-keeping constraint (8) is applied only at discrete sample points and treated as a soft constraint, minor violations of the station-keeping window are to be expected.

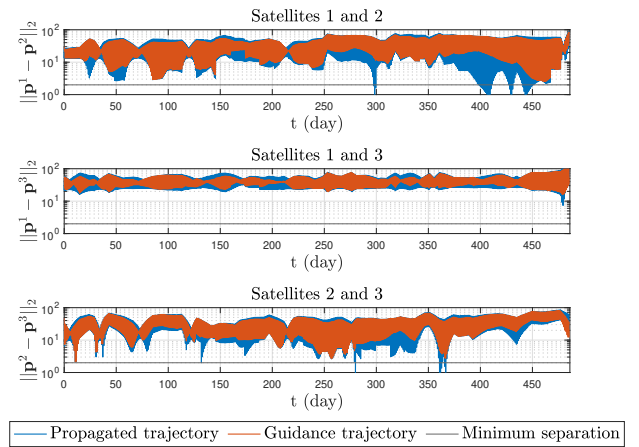
Figure 6 shows the cumulative Δv in the EW and NS directions for each of the three satellites over a 500 day period. The annual Δv values in the EW direction are $1.3 \frac{m}{s}$, $1.3 \frac{m}{s}$, and $1.3 \frac{m}{s}$ in for the first 365 days, and $1.4 \frac{m}{s}$, $1.4 \frac{m}{s}$, and $1.6 \frac{m}{s}$ for the last 365 days. In the NS direction, the annual Δv values are $50.7 \frac{m}{s}$, $49.7 \frac{m}{s}$, and $50.7 \frac{m}{s}$ in for the first 365 days, and $54.6 \frac{m}{s}$, $54.4 \frac{m}{s}$, and $54.3 \frac{m}{s}$ for the last 365 days. Note that compared to the single-satellite station-keeping problem, the Δv penalty incurred by collocating three satellites in the same station keeping window is small.

VI. CONCLUSION

A NMPC strategy employing SCP was presented for satellite station keeping and collocation for satellites with



(a) Proposed method.



(b) Baseline method.

Fig. 4: Separation distance between each pair of satellites for 3 satellite collocation over 500 day period.

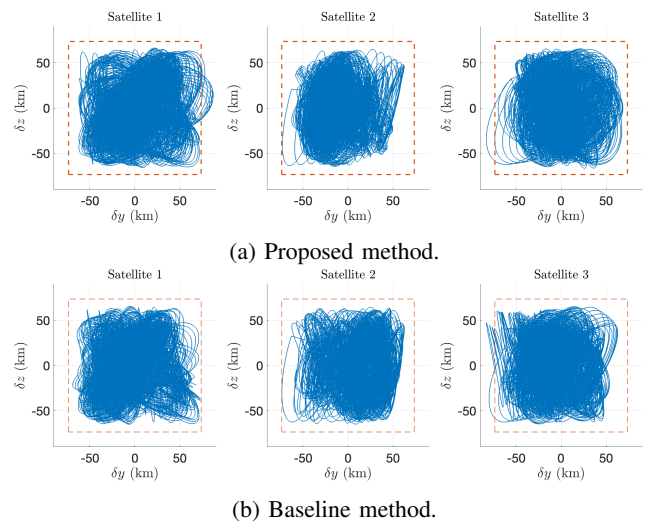


Fig. 5: Satellite position relative to the center of the station-keeping window, resolved in \mathcal{F}_H (blue) for 3 satellite collocation over 500 day period, with station-keeping window boundary (orange).

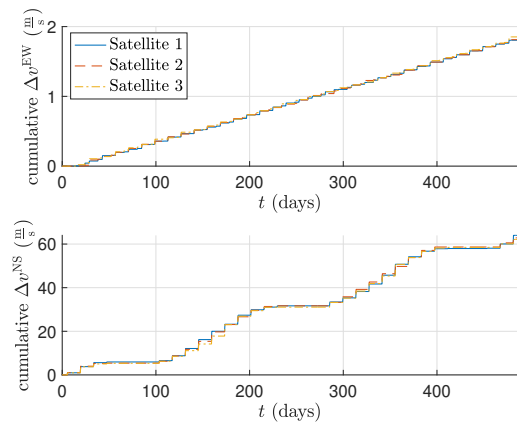


Fig. 6: Cumulative control input in EW and NS directions for 3 satellite collocation over 500 day period.

high-thrust impulsive propulsion systems. Time dilation was used to make thruster firing time a free variable. An isoperimetric constraint reformulation was used to enforce a pairwise satellite-separation constraints between sample points in discrete time. The proposed NMPC policy provides an accurate prediction model that enables station-keeping maneuvers with infrequent feedback. The policy can be extended to handle the harder problem of collocating multiple satellites within a single station-keeping window with the same infrequent high-thrust control and infrequent feedback. The resulting trajectory is locally fuel-optimal and uses the entire station-keeping window for fuel-efficient performance.

REFERENCES

- [1] E. M. Soop, *Handbook of geostationary orbits*. Springer Science & Business Media, 1994, vol. 3.
- [2] M. Eckstein and A. Leibold, "Autonomous station-keeping of geostationary satellites," *Spacecraft Pointing and Position Control, AGARD-AG-26*, 1981.
- [3] T. N. Edelbaum, "Optimum low-thrust rendezvous and station keeping," *Journal of Spacecraft and Rockets*, vol. 40, no. 6, pp. 960–965, 2003.
- [4] R. J. Caverly, S. D. Cairano, and A. Weiss, "Electric satellite station keeping, attitude control, and momentum management by mpc," *IEEE Transactions on Control Systems Technology*, vol. 29, no. 4, pp. 1475–1489, 2021.
- [5] C. Gazzino, C. Louembet, D. Arzelier, N. Jozefowicz, D. Losa, C. Pittet, and L. Cerri, "Integer programming for optimal control of geostationary station keeping of low-thrust satellites," *IFAC-PapersOnLine*, vol. 50, no. 1, pp. 8169–8174, 2017, 20th IFAC World Congress.
- [6] A. Sukhanov and A. Prado, "On one approach to the optimization of low-thrust station keeping manoeuvres," *Advances in Space Research*, vol. 50, no. 11, pp. 1478–1488, 2012.
- [7] A. Garulli, A. Giannitrapani, M. Leomanni, and F. Scortecchi, "Autonomous low-earth-orbit station-keeping with electric propulsion," *Journal of guidance, control, and dynamics*, vol. 34, no. 6, pp. 1683–1693, 2011.
- [8] D. Losa, "High vs Low Thrust Station Keeping Maneuver Planning for Geostationary Satellites," Theses, École Nationale Supérieure des Mines de Paris, Feb. 2007, financement d'Alcatel Alenia Space AAS. [Online]. Available: <https://pastel.hal.science/tel-00173537>
- [9] F. J. de Bruijn, S. Theil, D. Choukroun, and E. Gill, "Geostationary satellite station-keeping using convex optimization," *Journal of Guidance, Control, and Dynamics*, vol. 39, no. 3, pp. 605–616, 2016.

- [10] I. Beigelman and P. Gurfil, "Optimal geostationary satellite collocation using relative orbital element corrections," *Journal of Spacecraft and Rockets*, vol. 46, no. 1, pp. 141–150, 2009.
- [11] C. Rajasingh, "On the collision hazard of colocated geostationary satellites at 19 west," *GSOC IB*, pp. 89–01, 1989.
- [12] S. D'Amico and O. Montenbruck, "Proximity operations of formation-flying spacecraft using an eccentricity/inclination vector separation," *Journal of Guidance, Control, and Dynamics*, vol. 29, no. 3, pp. 554–563, 2006.
- [13] F. J. de Bruijn, S. Theil, D. Choukroun, and E. Gill, "Collocation of geostationary satellites using convex optimization," *Journal of Guidance, Control, and Dynamics*, vol. 39, no. 6, pp. 1303–1313, 2016.
- [14] D. Malyuta, T. Reynolds, M. Szmuk, M. Mesbahi, B. Acikmese, and J. M. Carson, "Discretization performance and accuracy analysis for the rocket powered descent guidance problem," in *AIAA Scitech 2019 Forum*, 2019, p. 0925.
- [15] A. G. Kamath, P. Elango, Y. Yu, S. Mceowen, G. M. Chari, J. M. Carson III, and B. Açıkmeşe, "Real-time sequential conic optimization for multi-phase rocket landing guidance," *IFAC-PapersOnLine*, vol. 56, no. 2, pp. 3118–3125, 2023.
- [16] F. Messerer, K. Baumgärtner, and M. Diehl, "Survey of sequential convex programming and generalized gauss-newton methods," *ESAIM: Proceedings and Surveys*, vol. 71, pp. 64–88, 2021.
- [17] D. Malyuta, T. P. Reynolds, M. Szmuk, T. Lew, R. Bonalli, M. Pavone, and B. Açıkmeşe, "Convex optimization for trajectory generation: A tutorial on generating dynamically feasible trajectories reliably and efficiently," *IEEE Control Systems Magazine*, vol. 42, no. 5, pp. 40–113, 2022.
- [18] P. Elango, D. Luo, A. G. Kamath, S. Uzun, T. Kim, and B. Açıkmeşe, "Successive convexification for trajectory optimization with continuous-time constraint satisfaction," 2024. [Online]. Available: <https://arxiv.org/abs/2404.16826>
- [19] S. Uzun, P. Elango, A. G. Kamath, T. Kim, and B. Acikmese, "Successive convexification for nonlinear model predictive control with continuous-time constraint satisfaction," 2024. [Online]. Available: <https://arxiv.org/abs/2405.00061>
- [20] J. B. Rawlings, D. Q. Mayne, M. Diehl *et al.*, *Model predictive control: theory, computation, and design*. Nob Hill Publishing Madison, WI, 2017, vol. 2.
- [21] M. Szmuk, T. P. Reynolds, and B. Açıkmeşe, "Successive convexification for real-time six-degree-of-freedom powered descent guidance with state-triggered constraints," *Journal of Guidance, Control, and Dynamics*, vol. 43, no. 8, pp. 1399–1413, 2020.
- [22] C. Gazzino, D. Arzelier, L. Cerri, D. Losa, C. Louembet, and C. Pittet, "Solving the minimum-fuel low-thrust geostationary station keeping problem via the switching systems theory," 2017. [Online]. Available: <https://api.semanticscholar.org/CorpusID:3488311>
- [23] X. Xu and P. Antsaklis, "Optimal control of switched systems based on parameterization of the switching instants," *IEEE Transactions on Automatic Control*, vol. 49, no. 1, pp. 2–16, 2004.
- [24] Q. Lin, R. Loxton, and K. L. Teo, "The control parameterization method for nonlinear optimal control: A survey," *Journal of Industrial and Management Optimization*, vol. 10, no. 1, pp. 275–309, 2014. [Online]. Available: <https://www.aims sciences.org/article/id/371849ed-608d-4e1a-9250-2ee3d01d59c1>
- [25] "General mission analysis tool (GMAT) mathematical specifications," NASA Goddard Space Flight Center, Tech. Rep., 2018.
- [26] R. Frick and T. Garber, "Perturbations of a synchronous satellite," The RAND Corporation, Tech. Rep., 1962.
- [27] B. Bucha and J. Janák, "A MATLAB-based graphical user interface program for computing functionals of the geopotential up to ultra-high degrees and orders," *Computers & Geosciences*, vol. 56, pp. 186–196, 2013.
- [28] D. Drusvyatskiy and A. S. Lewis, "Error bounds, quadratic growth, and linear convergence of proximal methods," *Mathematics of Operations Research*, vol. 43, no. 3, pp. 919–948, 2018.
- [29] T. Reynolds, D. Malyuta, M. Mesbahi, B. Acikmese, and J. M. Carson, "A real-time algorithm for non-convex powered descent guidance," in *AIAA Scitech 2020 Forum*, 2020, p. 0844.
- [30] H. G. Bock and K.-J. Plitt, "A multiple shooting algorithm for direct solution of optimal control problems," *IFAC Proceedings Volumes*, vol. 17, no. 2, pp. 1603–1608, 1984.